4308 *Organometallics* **2009,** *28,* 4308–4315
DOI: 10.1021/om9003253

ORGANOMETALLICS
Article

# Multidecker Sandwiches of Silicon−Carbon Clusters

E. N. Koukaras and A. D. Zdetsis*

*Department of Physics, University of Patras, GR-26500 Patras, Greece*

*Received April 27, 2009*

It is shown by *ab initio* density functional theory calculations that hydrogenated silicon−carbon clusters, in particular of the form $Si_3C_2H_2$, can generate stable organometallic multidecker sandwiches in which transition metal centers, such as Co and Fe, bridge $Si_3C_2H_2$ rings. These multidecker sandwiches are fully homologous and isolobal to the well-known similar metalocarborane sandwiches. This is in full agreement with the isolobal analogy between $Si_{n-2}C_2H_2$ clusters and the corresponding isovalent carboranes $C_2B_{n-2}H_n$, $n \geq 3$, known as the "boron connection". The interplanar binding energy of these sandwiches between successive decks increases as the number of decks increases, suggesting that even larger multideckers will also be very stable. Such organometallic species could be proven very important for chemical and technological applications, which could be integrated with current semiconductor technologies. With this perspective it is furthermore illustrated that by modifying the bridging transition metal or the multidecker linking method, such multidecker sandwiches could be tuned to exhibit specific electronic, optical, and magnetic properties. In addition, due to the chemical similarity provided by the "boron connection", it would be expected that most of the vital properties, capacities, and applications of the organometallic carboranes, metallaboranes, and metallacarboranes, in particular as building blocks (synthons) of more complex systems, could be transferable to the corresponding isolobal metal−silicon−carbon structures.

## 1. Introduction

Silicon, carbon, and silicon−carbon clusters, cluster assembled materials, and nanostructures in addition to their fundamental significance for chemistry, physics, and materials science are also of vital importance for technological and chemical applications in nanotechnology, biotechnology, and ceramics industry (this is particularly true for SiC). Composite metal−silicon clusters are widely known, especially as (transition) metal-embedded or (transition) metal-adsorbed silicon clusters.[1−5] Although small silicon carbon clusters have been well studied for several years,[6−8] metallic-SiC (and metallic-C) clusters are only known recently[9] mainly as models or subunits of larger systems, through their role in the production of carbon and silicon−carbon nanotubes, nanorods, and nanowires.[9,10] For instance, Zhao et al.[9] have examined silicon carbide nanotubes functionalized by transition metal atoms, while Terrones et al.[10] prepared SiC nanofibers by chemical vapor deposition (CVD), using carbon and silicon powders and hydrogen as a reactant gas with transition metal catalysts (Fe, Cr, or Ni). As we can see, transition metals are instrumental for such complex systems,[1−5,9,10] and so is hydrogen.

Another parallel and equally successful direction and approach for developing building blocks of functionalized and "functionalizable" complex systems (as, for instance, double- and multidecker metal−semiconductor sandwiches[11−13]) is through the methods and techniques of organometallic chemistry.[14] Silicon has long held a privileged status in organic synthesis. Organosilicon chemistry has matured substantially over the course of the past decade, and new methods have been developed for both the introduction of silicon groups and for chemical manipulation of those groups.[14] Organosilicon chemistry is an area of rapid expansion,[14] of almost comparable growth and importance to organoboron chemistry. These two fields are not totally

*Corresponding author. E-mail: zdetsis@upatras.gr.

(1) Beck, S. M. J. *Chem. Phys.* **1987**, *87*, 4233. Beck, S. M. J. *Chem. Phys.* **1989**, *90*, 6306.
(2) Hiura, H.; Miyazaki, T.; Kanayama, T. *Phys. Rev. Lett.* **2001**, *86*, 1733.
(3) Kumar, V.; Kawazoe, Y. *Phys. Rev. Lett.* **2001**, *87*, 045503.
(4) Kumar, V. *Comput. Mater. Sci.* **2006**, *36*, 1.
(5) Koukaras, E. N.; Garoufalis, C. S.; Zdetsis, A. D. *Phys. Rev. B* **2006**, *73*, 235417. Zdetsis, A. D. *Phys. Rev. B* **2007**, *75*, 085409.
(6) Mühlhäuser, M.; Froudakis, G. E.; Zdetsis, A. D.; Peyerimhoff, S. D. *Chem. Phys. Lett.* **1993**, *204*, 617. Froudakis, G. E.; Zdetsis, A. D.; Mühlhäuser, M.; Engels, B.; Peyerimhoff, S. D. *J. Chem. Phys.* **1994**, *101*, 6790.
(7) Zdetsis, A. D.; Engels, B.; Hanrath, M.; Peyerimhoff, S. D. *Chem. Phys. Lett.* **1999**, *302*, 288.
(8) Zhao, J.; Ding, Y. *J. Phys. Chem. C* **2008**, *112*, 2558–2564.
(9) Terrones, M.; Grobert, N.; Olivares, J. *Nature* **1997**, *388*, 52.
(10) Stephan, M.; Müller, P.; Zenneck, U.; Pritzkow, H.; Siebert, W.; Grimes, R. N. *Inorg. Chem.* **1995**, *34*, 2058.
(11) Bluhm, M.; Pritzkow, H.; Siebert, W.; Grimes, R. N. *Angew. Chem., Int. Ed.* **2000**, *39*, 4562.
(12) Edwin, J.; Whiteley, M. W.; Herter and, W.; Siebert, W. *J. Organomet. Chem.* **1990**, *394*, 329.
(13) Fessenbecker, A.; Attwood, M. D.; Bryan, R. F.; Grimes, R. N.; Woode, M. K.; Stephan, M.; Zenneck, U.; Siebert, W. *Inorg. Chem.* **1990**, *29*, 5157.
(14) Brook, M. A. *Silicon in Organic, Organometallic, and Polymer Chemistry*; John Wiley & Sons: New York, 2000.

 Published on Web 07/09/2009 

unrelated. Zdetsis[15−17] in a series of papers has demonstrated that the silicon cluster and borane dianions $(Si_n)^{2-}$−$(B_nH_n)^{2-}$ as well as the pairs of hydrogenated SiC clusters and the corresponding isovalent carboranes $Si_{n-2}C_2H_2$−$C_2B_{n-2}H_n$ are fully analogous and isolobal, at least for $n = 3-8$. This analogy could significantly contribute toward the design and functionalization of novel metal−silicon−carbon structures, from the knowledge of similar structures from metallaborane and metallacarborane chemistry. This is the direction pursued in the present paper.

As Grimes[18,19] stated more than 10 years ago, "a prominent theme of organometallic synthesis is the targeting of research toward specific goals, including the development of new types of smart materials". After so many years, these fruitful ideas and concepts have been (and continue to be) justified with well-known results and products. One of the most instrumental tools in this synthesis is the isolobal principle,[20] which reveals interconnections between presumably unrelated molecules.

Although the present work deals with no direct applications, this is also a prominent theme of the present investigation, in which some very well-known[18,19] and well-tested examples from metallacarborane chemistry are related through the isolobal "boron connection"[15−17] to predict the possible synthesis of corresponding metal−silicon−carbon multidecker sandwich complexes. These complexes could presumably be used as building blocks for possible new metal−semiconductor composite structures.

In multidecker carboranes or multidecker sandwiches the carborane ligands are mainly cyclopentacarboranes of the type $C_2B_3H_3$, forming $\eta^5$-face bonding, acting as electron donors to the metal atoms. The choice of carboranes instead of hydrocarbon rings abets electron sharing in the metal−ligand binding due to the lower electronegativity of boron (compared to carbon). Multidecker sandwiches can be grown by adding more decks. They are linked either directly or by a linking compound such as phenylene, thus forming oligomers, and finally they can be linked to form two-dimensional sheet polymers.[18,19] Their electronic and magnetic properties can be fine-tuned via adjustment of the number of layers, by proper selection of the interlayer transition metals, and by using different combinations of transition metals in the same sandwich. By doing so, the compounds can range from conducting to semiconducting and from dielectric to paramagnetic.

In the present investigation, in full analogy with the metallacarborane sandwiches, we build similar isovalent silicon−carbon structures and calculate their structural and electronic properties, for each pair of structures in parallel, paying special attention to the anticipated isolobal property. The results of the calculations and comparisons are discussed in Section 3, after a short description of the methods and techniques of the calculations in Section 2. The conclusions of this work are summarized in Section 4.

## 2. Technical Details of the Calculations

All of the calculations were performed within the density functional theory (DFT). The geometry optimizations were initially performed employing the gradient-corrected BP86 functional[21] without any symmetry constraints. The resulting structures were subsequently symmetrized (wherever possible) and reoptimized making use of the hybrid, three-parameter, functional of Becke, Lee, Yang, and Parr (B3LYP).[22] Previous work has shown[5,15−17] that, for the case of silicon and silicon−carbon clusters, B3LYP gives quite accurate structural and energetic results, comparable in most cases to those obtained by coupled cluster theory. This includes silicon clusters containing transition metals[5] (at least 3d transition metals).

The initial geometries, besides the ones intuitively suggested as best and worse case choices, were obtained by proper bond (length and angle) scaling of the corresponding metallacarboranes. These geometries were further modified and altered in many different ways (including modifications of the rotational and bending angles between the various layers) and by considering several spin alternatives. All these alterations and modifications (leading to low or no symmetry structures) verify that the planes of the structures' layers (of metallacarboranes and metal−silicon−carbon sandwiches) are not parallel to each other but rather form angles, depending on the transition metal, the number of decks, and the type of internal (esoteric) decks. In order to ensure that the structures obtained correspond at least to a very low energy minimum (near ground state structures), many different configurations were taken into account. Initial geometry configurations were derived from manipulation of the inner decks, using various planar and nonplanar structures, as well as the more tedious and laborious relative rotation of all decks around the Fe−Fe axis (see Figure 1). In addition, we have examined different initial angles between the planes of the decks. Frequency calculations have further verified that all these structures are, at least, low-energy local minima. Tight convergence criteria were placed for the maximum norm of the Cartesian gradient (up to $10^{-4}$ au), for the SCF energy (up to $10^{-7}$ H), and for the one-electron density (rms of the density matrix up to $10^{-7}$). For all calculations the triple-$\zeta$ quality TZVP[23] basis set was used. In order to ensure the correct electronic occupation, triplet states of the structures were examined as well, while in many cases a (pseudo-Fermi) occupation number thermal smearing procedure was employed. These calculations were performed with the TURBOMOLE[24] program package. The same package was also used for the Roby−Davidson−Heinzmann−Ahlrichs[25] (RDHA) population analysis calculations based on occupation numbers of modified atomic orbitals.[25]

The charge assignment of the atomic centers was calculated employing the quantum theory of atoms in molecule[26] (QTAIM) using the AIMall[26] program. The QTAIM method successfully treated the transition metal atoms (which were "problematic" with methods such as Mulliken population

(15) Zdetsis, A. D. *J. Chem. Phys.* **2007**, *127*, 014314. Zdetsis, A. D. *J. Chem. Phys.* **2007**, *127*, 244308.
(16) Zdetsis, A. D. *J. Chem. Phys.* **2008**, *128*, 184305. Zdetsis, A. D. *J. Phys. Chem. A* **2008**, *112*, 5712.
(17) Zdetsis, A. D. *Inorg. Chem.* **2008**, *47*, 8823. Zdetsis, A. D. *J. Chem. Phys.* **2009**, *130*, 064303.
(18) Grimes, R. N. *Coord. Chem. Rev.* **1995**, *143*, 71. *Coord. Chem. Rev.* **2000**, *200*, 811.
(19) Grimes, R. N. *Appl. Organomet. Chem.* **1996**, *10*, 209.
(20) Hoffman, R. *Angew. Chem., Int. Ed. Engl.* **1982**, *21*, 711.
(21) Becke, A. D. *Phys. Rev. A* **1988**, *38*, 3098. Perdew, J. P. *Phys. Rev. B* **1986**, *33*, 8822.
(22) Stephens, P. J.; Devlin, F. J.; Chabalowski, C. F.; Frisch, M. J. *J. Phys. Chem.* **1994**, *98*, 11623.
(23) Schäfer, A.; Huber, C.; Ahlrichs, R. *J. Chem. Phys.* **1994**, *100*, 5829.
(24) *TURBOMOLE* (*version 5.6*); Universitat Karlsruhe, **2000**.
(25) Roby, K. R. *Mol. Phys.* **1974**, *27*, 81. Davidson, E. R. *J. Chem. Phys.* **1967**, *46*, 3320. Heinzmann, R.; Ahlrichs, R. *Theor. Chim. Acta* (*Berlin*) **1976**, *42*, 33. Ehrhardt, C.; Ahlrichs, R. *Theor. Chim. Acta* **1985**, *68*, 231.
(26) Keith. T. A. *AIMAll* (*Version 09.02.01*); **2009** (aim.tkgristmill.com). Bader, R. F. W. *Atoms in Molecules. A Quantum Theory*; Oxford University Press: Oxford, 1995. Keith, T. A. Ph.D. Thesis, McMaster University, **1993**.

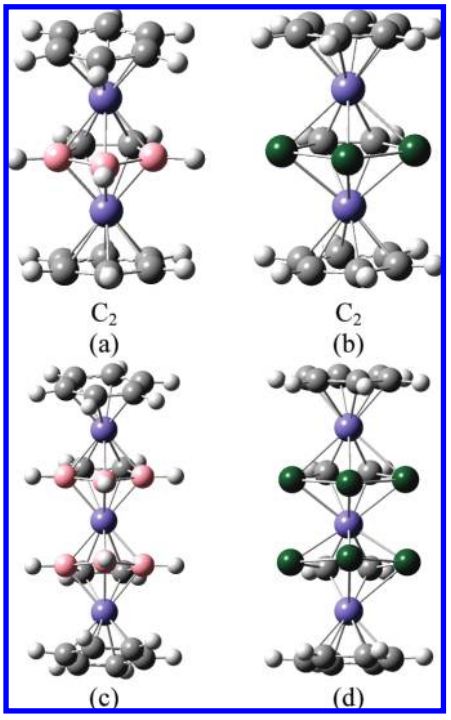


**Figure 1.** Structure of the (a) $C_{14}(BH)_3Fe_2H_{14}$ and (b) $C_{14}Si_3Fe_2H_{14}$ triple-decker sandwiches and the (c) $C_{16}(BH)_6Fe_3H_{16}$ and (d) $C_{16}Si_6Fe_3H_{16}$ tetradecker sandwiches. The structures of $C_{14}(BH)_3Co_2H_{14}$, $C_{14}Si_3Co_2H_{14}$, $C_{16}(BH)_6Co_3H_{16}$, and $C_{16}Si_6Co_3H_{16}$ are in general similar.

analysis), although the computationally more costly first-order Promega integration method[26] was needed (instead of the Proaim algorithm[26]) for the integration on the atomic basins. The geometry optimization calculations were performed using the Turbomole[24] program package. The Gaussian 03 package[27] was used for the spin-polarized calculations.

In order to further facilitate the analysis of the electronic properties, we have developed a simple code to calculate the crystal orbital overlap population[28] (COOP) diagrams (as described in ref 5) as well as the total and partial density of states. The density-of-states (DOS) curves were derived by a suitable Gaussian broadening of the energy levels.

## 3. Results and Discussion

In this work we examine triple- and tetradecker sandwiches for two different choices of the linking transition metal, TM = Fe and Co, and for two different cases of inner decks, specifically five-membered boron−carbon rings and five-membered silicon−carbon rings. The electronic and especially the magnetic properties of the compounds have a strong dependence on the choice of the transition metal, as will be shown. However, the type of transition metal does not have a significant impact on the structure of the compounds.

Regarding the nomenclature of the structures, throughout this work, besides the full elaborated notation, we will be using sometimes for brevity (in particular in table headings and figure captions) the alternative more compact abbreviated stoichiometry form of the compounds. Thus for example, the triple-decker $(\eta^6\text{-}C_6H_6)Fe(\eta^5\text{-}C_2Si_3H_2)Fe(\eta^6\text{-}C_6H_6)$ will be denoted in such cases simply as $C_{14}Si_3Fe_2H_{14}$, while the corresponding carborane structure will be denoted by $C_{14}(BH)_3Fe_2H_{14}$ to bring up the analogy and ease comparison.

**3.1. Comparison of Structural and Cohesive Properties.** In Figure 1 we show a side by side view of the carborane- and silicon−carbon-based triple-decker (Figure 1a,b) and tetradecker (Figure 1c,d) sandwiches for the case of Fe as the linking transition metal. The inner (middle) decks are cyclopenta (a) $C_2B_3H_5$ and (b) $C_2Si_3H_2$ rings, which are linked by Fe atoms to the two capping arenes.

For TM = Co in general the structures are pretty much similar with the exception of "interplanar" angles, which can show a variation up to 15° from the corresponding angles with TM = Fe. Also for the silicon−carbon-based tetradecker in the case of TM = Co there is a significant 1−1 bonding between the central silicon atoms of the two inner decks. A similar but much less pronounced bonding occurs with the borane atoms in the corresponding carborane tetradecker. This "additional" bonding is reflected in the cohesive properties of the TM = Co tetradeckers.

The calculated binding (atomization) energies (BE) of the structures are given in Table 1. The values correspond to DFT calculations at the B3LYP level of theory, using the TZVP basis set. As we can see in Table 1, although the tripledecker BEs for TM = Fe and TM = Co are comparable, the tetradecker BEs for TM = Co are higher. This must be related with the additional "interplanar" bonding in the tetradeckers, mentioned above. What is even more important is that in all cases the binding energy increases as the number of decks increases.

The BE of the structures account for the binding of the structures as a whole. What is also of interest is the binding between decks. For this reason, to quantify the "interdecker" binding, we define the decker binding energy (DBE) by the following relation:

$$\mathrm{DBE} = E(\mathrm{d}_1) + E(\mathrm{d}_2) + \cdots + E(\mathrm{d}_N) + (N-1) \times E(\mathrm{TM}) - E(\mathrm{multidecker}) \quad (1)$$

where $N$ is the number of decks that make up the multidecker structure, and $E(\mathrm{d}_1)$, $E(\mathrm{d}_2)$, and $E(\mathrm{d}_N)$ are the energies of the first, second, and $N$th decks, correspondingly, calculated separately. $E$(TM) is the energy of the linking transition metal and $E$(multidecker) is the energy of the sandwich. The decker binding energy may be conceived as analogous to the atomization energy with the difference that instead of "breaking" the structure in atoms, one does so in decks. Values of the DBE for both triple- and tetradeckers are also given in Table 1 (values correspond to calculations employing the B3LYP functional using the TZVP basis set).

The structures under consideration have sufficiently high binding energies and are well bound (the BP86 functional gives even larger binding energies and smaller HOMO−LUMO gaps). The HOMO−LUMO (HL) gap is larger for the carborane-based sandwiches. Although the BE of the carborane-based structures is higher than the corresponding silicon−carbon-based ones, we find that this ordering is reversed in the case of the vertical decker binding energy, VDBE, for non-relaxed decks, defined as in eq 1, but with the energies $E(\mathrm{d}_1)$, ..., $E(\mathrm{d}_N)$ corresponding to the decks 1, ..., $N$ *not* having undergone a geometry optimization. This difference (in VDBE) is

(27) Frisch, M. J.; et al. *GAUSSIAN 03, Revision C.02*; Gaussian, Inc.: Wallingford, CT, 2004.
(28) Hughbanks, T.; Hoffmann, R. *J. Am. Chem. Soc.* **1983**, *105*, 3528.

**Table 1. Binding Energy, BE, of Triple-Decker Sandwiches, the HOMO−LUMO Gap, the Vertical and Adiabatic Decker Binding Energy, VDBE and ADBE, and the DBE Differences between Triple- and Tetradeckers (ΔVDBE, ΔADBE), As Calculated Using the B3LYP Functional[a]**

| | | B3LYP/TZVP | | | | | | |
|---|---|---|---|---|---|---|---|---|
| structure | spin | energy (H) | HL (eV) | BE (eV) | VDBE (eV) | ΔVDBE (eV) | ADBE (eV) | ΔADBE (eV) |
| $C_{14}(BH)_3Fe_2H_{14}$ | s (s) | −3145.377 | 3.45 | 164.54 (209.76) | 7.03 (11.77) | 4.74 | 6.69 (9.62) | 2.93 |
| $C_{14}Si_3Fe_2H_{14}$ | s (s) | −3937.375 | 2.89 | 148.71 (178.16) | 7.42 (13.26) | 5.84 | 7.08 (8.70) | 1.62 |
| $C_{14}(BH)_3Co_2H_{14}$ | t (d) | −3383.514 | 3.24 | 164.95 (210.12) | 7.33 (12.19) | 4.86 | 7.10 (9.98) | 2.88 |
| $C_{14}Si_3Co_2H_{14}$ | t (d) | −4175.495 | 1.43 | 148.67 (180.53) | 8.14 (14.85) | 6.71 | 7.03 (11.07) | 4.04 |

[a] All structures are well bound. The values in parentheses correspond to the tetradeckers.

even larger when calculating the VDBE per number of bound decks (the number of pair bound decks is $N-1$, with $N$ being the number of decks). The calculated VDBE/($N-1$) values are 3.92 eV for $C_{16}(BH)_6Fe_3H_{16}$, but 4.42 eV for $C_{16}Si_6Fe_3H_{16}$. For the corresponding triple-deckers the values become 3.51 and 3.71 eV, accordingly.

In this case the reversal in the energetic ordering is apparently due to the structural relaxation of the individual decks involved in the calculation of the adiabatic quantities, since the silicon−carbon decks refrain from a planar layout in the absence of the remaining multidecker structure (and especially the capping transition metals). This suggests that the carborane-based structures have a stronger binding as a whole and stronger intraplanar ("intradecker") binding than the silicon−carbon-based ones, while the silicon−carbon multideckers exhibit a stronger interplanar ("interdecker") binding between the decks. However, when examining the adiabatic decker binding energy, ADBE (as defined in eq 1, with the energies $E(d_1)$, ..., $E(d_N)$ corresponding to the decks $1-N$ having undergone a geometry optimization), we find the carborane-based structures to have higher values. Yet, in every case, all of the energetic quantities examined here increase with the number of decks in the sandwiches (a trend that continues at least up to $N=6$). With all cohesive criteria from all silicon−carbon-based structures in Table 1 the TM = Co tetradeckers are best bound. When considering the growth from triple- to tetradeckers, based on ΔVDBE and ΔADBE, the TM=Co tetradeckers are favored even more compared to all structures including the corresponding carborane-based multideckers.

**3.2. Orbital Characteristics of TM = Fe Triple-Deckers.** In Table 2 we list the frontier and near-frontier orbital energies for the carborane- and silicon−carbon-based triple-decker sandwiches, obtained at the DFT/B3LYP level.

In the same table we also list the corresponding symmetry (irreducible representations) of the orbitals. As we can see in the table, a comparison of the listed values reveals that the criterion for similar orbital energies (and, as a result, of energy differences) is satisfied. Furthermore, even though the structures are of relatively low symmetry ($C_2$), we note that corresponding frontier (and near-frontier) orbitals belong to the same irreducible representations, and as shown in Figure 2, they are very much alike.

Thus, the basic criteria for the isolobal property[20] ("similarity" and symmetry of the corresponding orbitals) are satisfied. The similarities revealed in Figure 2, which extend to the near-frontier orbitals, are striking, suggesting that the compounds are clearly isolobal. The main difference in the orbitals is the slightly more pronounced lobes near the silicon atoms in the case of the silicon−carbon-based structures, relative to those around the boron atoms in the carborane-based structures. This is obviously related to the difference between Si lone pairs and B−H bonds.

**Table 2. Orbital Energies in Atomic Units (au) and Irreducible Representation (irrep) of the Frontier and Near-Frontier Orbitals for Carborane and Silicon−Carbon Triple-Deckers with Fe as the Linking Metal**

| $C_{14}(BH)_3Fe_2H_{14}$ | | $C_{14}Si_3Fe_2H_{14}$ | |
|---|---|---|---|
| orbital | energy/irrep | orbital | energy/irrep |
| LUMO+1 | −0.039/a | LUMO+1 | −0.046/a |
| LUMO | −0.040/b | LUMO | −0.052/b |
| HOMO | −0.168/b | HOMO | −0.160/b |
| HOMO−1 | −0.203/a | HOMO−1 | −0.175/a |
| HOMO−2 | −0.204/b | HOMO−2 | −0.196/b |

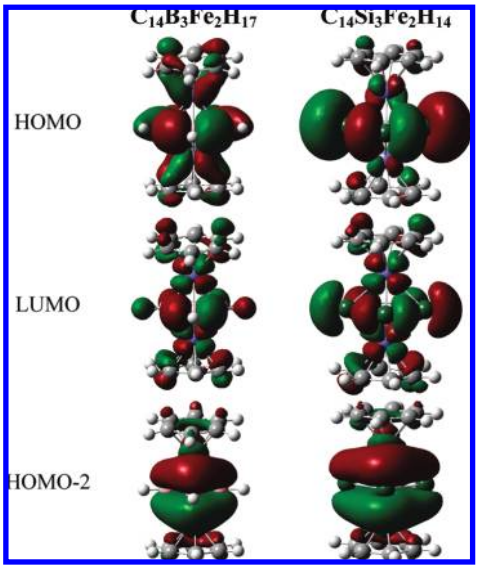


**Figure 2.** HOMO, LUMO, and HOMO−2 orbitals of the carborane- and silicon−carbon-based triple-deckers for the case of TM = Fe. All figures correspond to the same isovalue. The similarity in the orbital shape is apparent.

Another common characteristic for both silicon−carbon- and carborane-based species is alternating charges,[6,16,17] which in principle could be calculated by standard Mulliken population analysis (MPA) or RDHA population analysis based on modified atomic orbitals. The RDHA method has the additional advantage of allowing the calculation of multicenter-shared electron numbers, describing quantitatively the multicenter bonding, which is an additional characteristic of both isolobal species.[16,17] Concerning the charges of the atomic centers, neither MPA nor RDHA produces reliable and comparable results. The MPA method on these structures gives rather poor results, both quantitative and qualitative. The RDHA population analysis[25] reveals that there are significant multicenter-shared electron number (SEN) contributions to the atomic charges. If we

**Table 3. Charges of the Atomic Centers That Constitute the Inner Structure of the Triple-Decker Sandwiches As Calculated Using the QTAIM Method[26a]**

| | atomic charges | | | |
|---|---|---|---|---|
| atom | $C_{14}(BH)_3Fe_2H_{14}$ | $C_{14}Si_3Fe_2H_{14}$ | $C_{14}(BH)_3Co_2H_{14}$ | $C_{14}Si_3Co_2H_{14}$ |
| C(1) | −0.84 | −0.86 | −0.80 | −0.97 |
| C(2) | −0.84 | −0.86 | −0.80 | −0.97 |
| B/Si(1) | 1.05 (0.35) | 0.51 | 1.05 (0.34) | 0.67 |
| B/Si(2) | 0.46 (−0.23) | −0.21 | 0.54 (−0.18) | −0.44 |
| B/Si(3) | 1.05 (0.35) | 0.51 | 1.05 (0.33) | 0.68 |
| Fe/Co(1) | 0.81 | 0.62 | 0.72 | 0.63 |
| Fe/Co(2) | 0.80 | 0.62 | 0.72 | 0.63 |
| H(1) | −0.05 | −0.03 | −0.06 | −0.04 |
| H(2) | −0.05 | −0.03 | −0.06 | −0.04 |
| H(3) | −0.70 | | −0.72 | |
| H(4) | −0.70 | | −0.72 | |
| H(5) | −0.70 | | −0.72 | |
| inner deck net charge | −1.31 | −0.97 | −1.23 | −1.11 |

[a] Values in parentheses correspond to BH pairs. The atoms are numbered in accordance with Figure 3. The net charges of the middle (inner) deck are given in the last row.

want to study the atomic charges and the charge transfer involved, in particular in the presence of transition metal atoms (TMA), by more accurate methods we must consider methods such as QTAIM.[26] In Table 3 we give the assigned atomic charges as calculated employing the QTAIM, which is particularly important for the treatment of TMA. In the same table we list the atomic charges for the TM = Co triple-deckers to facilitate comparison. As we can see in Table 3, the charges of the B−H pairs (carborane-based structures) are lower (in almost all cases) compared to those of the corresponding silicon atoms (silicon−carbon-based structures). This is a result of the slightly lower electronegativity of silicon compared to boron (and hydrogen). Comparing the TM = Fe with the TM = Co structures we can see that the magnitude of the charges in the TM = Co silicon−carbon-based structures is larger compared to TM = FM. Exactly the opposite happens for the carborane-based structures. Comparing the silicon−carbon- and carborane-based structures for TM = Fe we find that the carbon atoms of the middle decks are negatively charged and of about the same value, while the Fe atoms of the silicon−carbon structure have a slightly lower positive charge.

The Fe atoms act as electron donors to the middle deck structure in both cases and with the same quantity of charge transfer; that is, the charge difference between all the silicon atoms (in the silicon−carbon structure) and all the BH pairs, $\Delta E_{Si-BH}$, has the same value as the charge difference between the Fe atoms of the two structures, $\Delta E_{Fe(SiC)-Fe(BC)}$.

We also note the existence of alternating charges on the atomic centers of the middle decks, which is more prominent in the silicon−carbon structure and is of the form C(−) Si(+)Si(−)Si(+)C(−). Alternating charges exist in the axial direction of the structures as well, which for the silicon−carbon structure is of the form Fe(+) middle_deck(−)Fe(+). Analogous results exist for the TM = Co structures. At the end of Table 3 we give the net charges of the middle decks of each triple-decker sandwich.

In addition to the alternating charges (similar in both types of structures), in Table 4 we have summarized some representative large-magnitude SENs for three- and four-center bonds in $C_{14}Si_3Fe_2H_{14}$ and $C_{14}(BH)_3Fe_2H_{14}$. As we can see in this table, the multicenter bonding in the two species, although slightly larger in $C_{14}(BH)_3Fe_2H_{14}$, is practically of the same magnitude. Also, it is clear from Table 4 that the contribution of Fe in the multicenter bonding is very significant and perhaps (by comparing to the corresponding non-Fe values) slightly stronger in $C_{14}Si_3Fe_2H_{14}$.

**Table 4. Comparison of Multicenter Bonding of $C_{14}Si_3Fe_2H_{14}$ and $C_{14}(BH)_3Fe_2H_{14}$ through Three- and Four-Center SENs[a]**

| $C_{14}B_3Co_2H_{17}$ | $C_{14}Si_3Co_2H_{14}$ |
|---|---|
| C(2)Si(1)Fe(1) = 0.37 | C(2)B(1)Fe(1) = 0.46 |
| Si(1)Si(2)Fe(1) = 0.32 | B(1)B(2)Fe(1) = 0.42 |
| C(2)Si(1)Si(2) = 0.30 | C(2)B(1)B(2) = 0.39 |
| C(1)Si(1)Si(2)Fe(2) = 0.23 | C(1)B(1)B(2)Fe(2) = 0.16 |
| C(2)Si(2)Fe(1)Fe(2) = 0.23 | C(2)Si(2)Fe(1)Fe(2) = 0.23 |
| C(1)Si(2)Si(3)Fe(2) = 0.16 | C(1)B(2)B(3)Fe(2) = 0.23 |

[a] The numbering of the atoms is according to Figure 3.

In Figure 4 we plot the DOS curve for the minimum energy triple-decker structures. The solid lines represent the total DOS. The dashed lines show the partial DOS (pDOS), and specifically the contribution to the DOS from the transition metal (Fe), from all the B/Si atoms, and from the central B/Si atom. The total DOS has remarkable similarities at least in the region of the Fermi and the near-Fermi level. At the Fermi level there are significant contributions from the Fe atoms (over 50%). A crystal orbital overlap population[28] (COOP) diagram analysis shows that these Fe-dominated states have a nonbonding character in both the silicon−carbon and the carborane structures (the overlaps taken are those of the Fe atoms with all the remaining atoms of the structures). The central boron and silicon atoms contribute significantly at this region. Especially for the case of silicon, the contribution reaches 50% at the HOMO−1 state.

At slightly lower energies, i.e., at the near-Fermi levels (−7.5 to −12 eV), the contributions from the Fe atoms are reduced. At this region the B and the Si atoms contribute in a very similar manner. In the immediate region after the Fermi level (−7.5 to −9.5) the Si atoms do not contribute to the states, while the B atoms contribute only slightly.

**3.3. Orbital Characteristics for the Co-linked Sandwiches.** As we mentioned earlier, the structures of the triple-decker and tetradecker sandwiches with Co as the linking transition metal are very similar to the corresponding structures with Fe, shown in Figure 1 (except for an angle difference up to 15° in the angle between the planes of the capping arenas). It can be anticipated that something similar happens for the electronic properties and the orbital characteristics in view of the isolobal analogy of the "boron connection".

Indeed, using Co atoms as the linking transition metal we once again find that the carborane-based and the silicon−carbon-

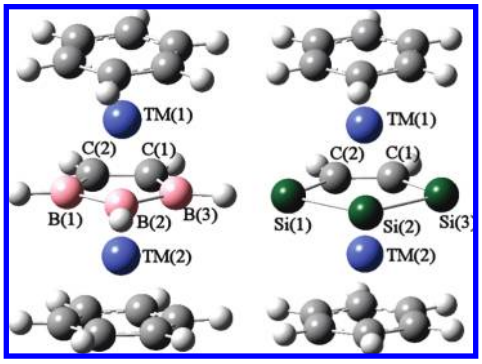


**Figure 3.** Numbering of the atoms of the inner structures used in Tables 3 and 4. The numbering of the hydrogen atoms of the middle deck starts from the hydrogen bonded to C(1) and increases counterclockwise. Bonding has been omitted for reasons of clarity.

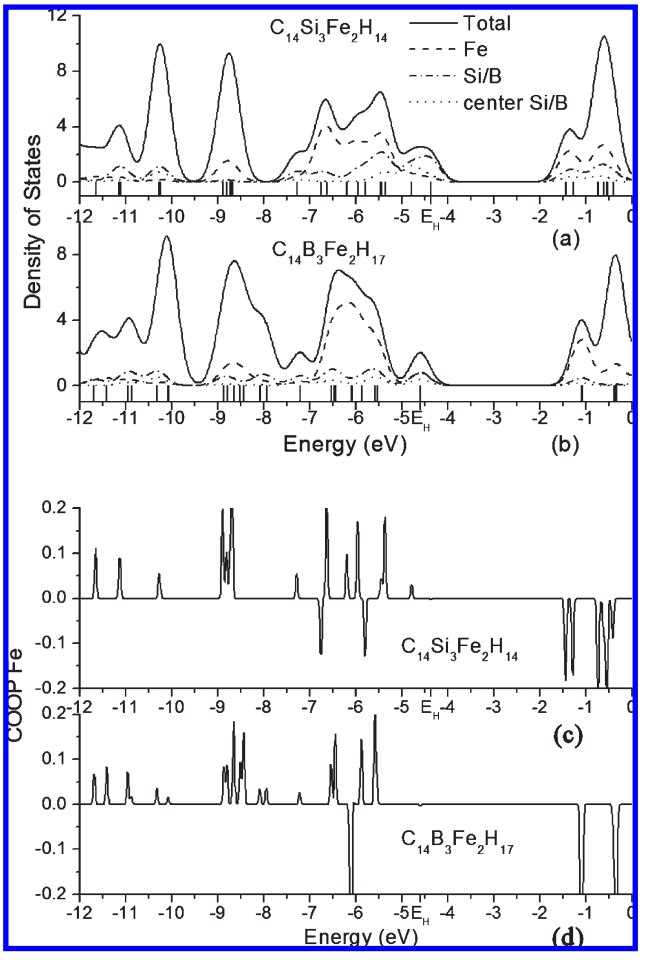


**Figure 4.** Density of states (DOS) and partial DOS of (a) $C_{14}Si_3Fe_2H_{14}$ and (b) $C_{14}(BH)_3Fe_2H_{14}$ and the crystal orbital overlap population (COOP) diagrams (c, d) of the Fe atom (overlaps taken are with all remaining atoms). Dotted lines correspond to the pDOS of the central Si/B atoms of the middle deck. Solid lines correspond to total density of states.

based triple-decker sandwiches are homologous and isolobal. In Table 5 we give the energies and the symmetry (irreducible representations) of the frontier and near-frontier orbitals. What is interesting is that there is a permutation between some of the (frontier and near-frontier) orbitals, as is shown in Figure 5.

**Table 5. Orbital Energies (in au) and Symmetries (irrep) of the Frontier and Near-Frontier Orbitals for Carborane and Silicon−Carbon Triple-Deckers with Co as the Linking Metal**

| $C_{14}B_3Co_2H_{17}$ | | $C_{14}Si_3Co_2H_{14}$ | |
|---|---|---|---|
| orbital | energy/irrep | orbital | energy/irrep |
| LUMO+1 | −0.039/b | LUMO+1 | −0.076/a |
| LUMO | −0.044/a | LUMO | −0.078/b |
| HOMO | −0.165/b | HOMO | −0.131/a |
| HOMO−1 | −0.169/b | HOMO−1 | −0.156/b |
| HOMO−2 | −0.181/a | HOMO−2 | −0.164/b |

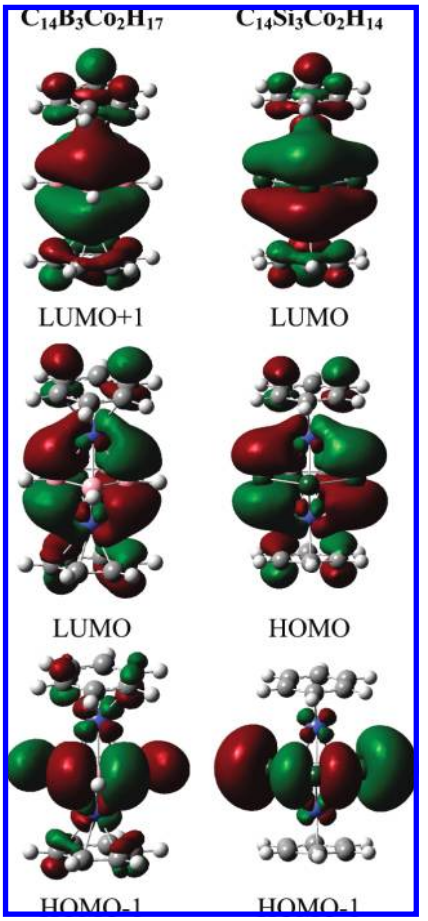


**Figure 5.** HOMO, LUMO, HOMO−1, and LUMO+1 orbitals of the carborane- and silicon−carbon-based triple-deckers for the case of TM = Co. All figures correspond to the same isovalue.

This is not uncommon[15b,17b] for isolobal species. In the present case the HOMO orbital of $C_{14}Si_3Co_2H_{14}$ corresponds to the LUMO of $C_{14}B_3Co_2H_{17}$.

An RDHA analysis shows, as in the case of TM = Fe, that there is considerable multiceneter bonding and also that there are significant multicenter contributions to the atomic charges. The QTAIM analysis of the triple-decker structures given in Table 2 reveals two main differences for the silicon−carbon structure compared to the TM = Fe case; first the carbon atoms of the central deck are more negatively charged, and second the charge distributions on the silicon atoms are more inhomogeneous.

As in the case of TM = Fe, we note the existence of alternating charges on the atomic centers of the middle deck, which is especially prominent in the silicon−carbon structure and is of the form C(−)Si(+)Si(−)Si(+)C(−). Alternating charges exist in the axial direction of the structures as well,

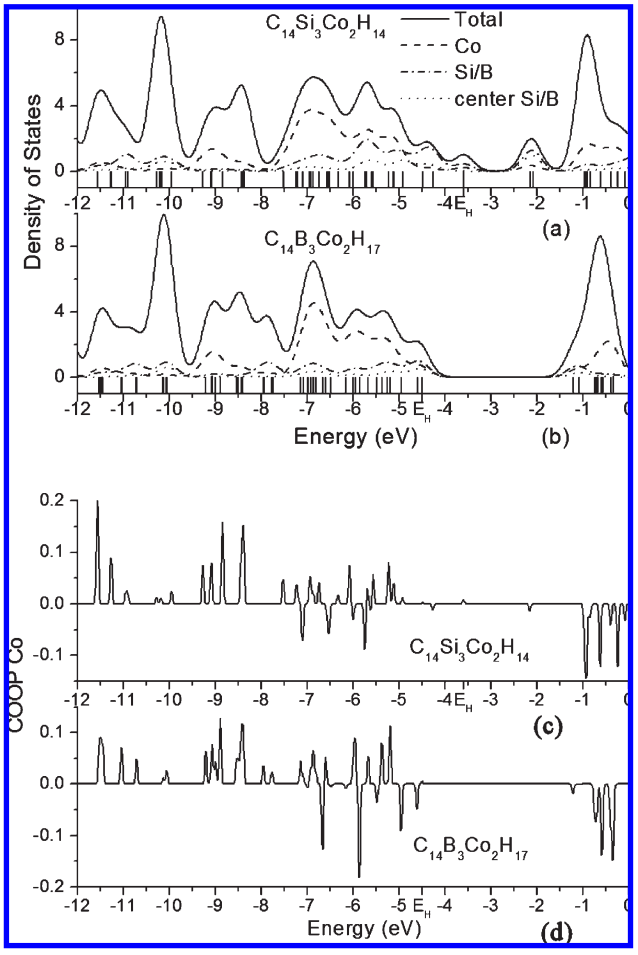


**Figure 6.** Density of states (DOS) and partial DOS of (a) $C_{14}Si_3Co_2H_{14}$ and (b) $C_{14}B_3Co_2H_{17}$ and the crystal orbital overlap population (COOP) diagrams (c, d) of the Co atom (overlaps taken are with all remaining atoms) for both cases. Dotted lines correspond to the pDOS of the central Si/B atoms of the middle deck. Solid lines correspond to total density of states.

which for the silicon−carbon structure is of the form Co-(+)middle_deck(−)Co(+).

In Figure 6 we have plotted the density of states for the minimum energy triple-decker structures.

The significantly smaller energy gap in the case of the silicon−carbon-based structure stands out. Both the LUMO and the HOMO (energy level near −3.6 eV) of this structure have a high contribution from the silicon atoms, specifically 45% and 65%, accordingly, while the HOMO−1 level has an even higher contribution of 85%. These contributions are slightly antibonding for the boron atoms and nonbonding for the silicon atoms. It is expected that the surface regions near the silicon atoms are prone to reactions. For both structures, the Co atoms have significant contributions (over 60%) in the immediate region after the Fermi level, specifically from −5 to −8 eV.

**3.4. Comparison of Magnetic Properties.** Our calculations on the carborane structures are in agreement with the experimental data of Grimes. Grimes performed[18,19] ESR measurements on carborane-based multideckers that incorporate Co as the deck-linking transition metal. In this case the multidecker structure is paramagnetic. We verify that by substituting BH by Si atoms, the compound remains paramagnetic, as it would be expected on the basis of a simple

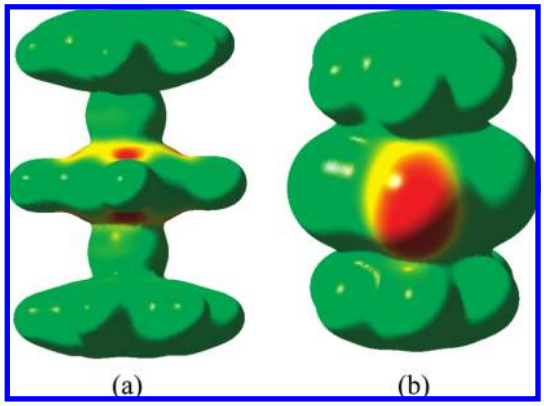


**Figure 7.** Spin density color-mapped isosurfaces of the electron density of the (a) $C_{14}B_3Co_2H_{17}$ and (b) $C_{14}Si_3Co_2H_{14}$ triple-deckers.

electron count. More specifically, the lowest energy structure for both the carborane- and silicon−carbon-based structures with TM = Co is a spin a triplet state. In Figure 7 we show the electron density with color mapping taken from the spin density at the isosurface. Areas shaded in red indicate a negative spin density (corresponding to an excess of beta electrons, with a minimum value of $-1.2 \times 10^{-2}$ for Figure 7a and $-2.6 \times 10^{-3}$ for Figure 7b), whereas areas shaded in green have uniform $\alpha$ and $\beta$ spin densities.

For the $C_{14}Si_3Co_2H_{14}$ structure, at the isovalue taken here, there are no clear regions of positive spin densities (excess of alpha). This is a result of the concentration of alpha electrons around the two Co atoms (which are internal to the whole structure). However we do find a significant concentration of beta electrons around the central Si atom.

For $C_{14}B_3Co_2H_{17}$, even though a lower isovalue was used, the beta electron regions are smaller, but are more extensive; that is, they are delocalized over the BH groups. Nevertheless, the beta regions are correlated with the B atoms, in a similar manner to $C_{14}Si_3Co_2H_{14}$ for Si atoms (specifically over the central Si atom). Thus, in both cases (carborane- and silicon−carbon-based structures) the two compounds exhibit *similar spin polarization*, with a higher electron delocalization in the carborane case. This higher electron delocalization can be seen in Figure 8.

In Figure 8 we have plotted the electron spin density at an isovalue of 0.005 for both structures. Here we can clearly see separate regions of alpha (blue) and beta (green) electrons. The middle deck separates the alpha electron regions centered on the Co atoms. In the case of $C_{14}B_3Co_2H_{17}$, the delocalization of the beta electrons throughout the central ring is evident, with a higher concentration around the B atoms. Furthermore, there are alpha spin regions between the B atoms. In the case of $C_{14}Si_3Co_2H_{14}$, we have much less delocalization, with the beta electrons region highly concentrated around the central Si atom of the central deck. An additional reason for the lack of beta regions in the electron density isosurfaces, in the case of carborane (Figure 7a), is the presence of the H atoms of the BH groups. The H atoms shield these regions. The lack of H atoms in the case of $C_{14}Si_3Co_2H_{14}$ (we have bare Si atoms) reveals this region rendering these structures significantly more chemically reactive, compared to $C_{14}B_3Co_2H_{17}$. This provides an additional bonding site between silicon−carbon-based

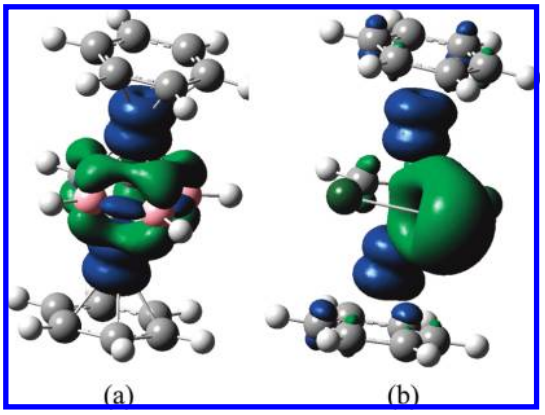


**Figure 8.** Electron spin density of the (a) $C_{14}B_3Co_2H_{17}$ and (b) $C_{14}Si_3Co_2H_{14}$ triple-deckers. Blue indicates alpha electron regions; green indicates beta electron regions.

multideckers and should facilitate the experimental synthesis of linked sandwich systems (like the ones proposed for carborane structures by Grimes[18]) in attempts to create 2D oligomer sheets from silicon−carbon-based multidecker building blocks (synthons). This localization of the silicon−carbon-based triple-decker sandwiches, especially around the silicon atoms (as opposed to the interior of the structure, where some delocalization exists) suggests that *linked* multideckers may not be conducting and should exhibit bulk *magnetic* properties, resulting from trapped unpaired electrons localized within the individual multidecker building blocks. This merits further investigation, as it may pave the road to a new class of silicon-containing organometallic multidecker materials that exhibit molecular ferromagnetism.

In Table 5 we present the spin polarizations for the Co and Si/B atoms of the triple-decker structures.

The Co atoms in both structures have approximately the same (high) spin density. The central B atom has double the spin density of the remaining two B atoms. In the silicon−carbon structure, the central Si atom has a significant spin density (−1), while that of the remaining Si atoms is negligible. This is in accord with our previous discussion. The remaining atoms in both structures have negligible spin polarizations, the values of which are all absolutely below 0.05.

**Table 6. Total Spin Density of the Triple-Decker Sandwiches**

| atom | $C_{14}B_3Co_2H_{17}$ | $C_{14}Si_3Co_2H_{14}$ |
|---|---|---|
| Co | 1.46 | 1.54 |
| Co | 1.46 | 1.54 |
| B/Si | −0.14 | 0.05 |
| B/Si | −0.14 | 0.05 |
| B/Si (central) | −0.21 | −1.00 |

## 4. Conclusions

In this work we have shown and predicted that novel organometallic silicon-based stable structures, such as multidecker sandwiches, can in principle be synthesized and hopefully operate analogously to the carborane-based sandwiches. On the basis of atomization energy and "decker binding energy" we have predicted and illustrated that larger multideckers would be stable, and in fact more stable, than the smaller ones.

We have also verified that by making use of the isolobal boron connection analogy and taking advantage of already existing well-known carborane-based structures and processes, we could in principle design (and hopefully synthesize) these novel organometallic silicon-based materials. This would be a practical application of the "boron connection". The silicon-based multidecker sandwich structures studied here exhibit similar, but not identical, properties to their corresponding (well-studied) carborane-based structures. The similarities between the two types of structures extend (but are not limited) to their symmetry, structural, and electronic properties. For the silicon−carbon structures, depending on the selected transition metal, the energy gaps can be adjusted within a wider range of values as a result of near-Fermi level states (frontier orbitals) with high contributions from the silicon atoms. The synthesis of linked silicon−carbon multidecker sandwiches could be further facilitated by the existence of additional linking regions present in these compounds compared to their corresponding carborane structures, and their spin dependence offers an added functionalization. In cases where the magnetic properties are of special interest, the silicon−carbon-based structures exhibit higher spin polarization with less delocalization and seem better suited as synthons for possible manufacturing of molecular magnetic materials.

We hope that the present work and the examples we have examined here will stimulate additional theoretical and experimental work along the same (guide)lines.